

CHAPTER IV

RESULTS AND DISCUSSION

4.1 Selectivity and Adsorption of *m*-CNB and *p*-CNB

Selectivity and adsorption of *m*-CNB and *p*-CNB on various adsorbents (NaX, CaX, BaX, NaY, CaY, KY, Al₂O₃, SiO₂, activated carbon and glass bead) are shown in Table 4.1. *m*-CNB/*p*-CNB selectivity of all zeolites is higher than one because the high acid strength zeolites having high electrostatic fields strongly interact with *m*-CNB more than *p*-CNB resulting in higher *m*-CNB adsorption than *p*-CNB (Leardsakulthong, 2008). *m*-CNB/*p*-CNB selectivity of Al₂O₃ is close to one because Al₂O₃ adsorbs about the same amount of both *m*- and *p*-CNB. Activated carbon has *m*-CNB/*p*-CNB selectivity less than one because *p*-CNB has higher polarity (its dipole moment is 2.83 of *p*-CNB compared to 3.73 of *m*-CNB). The *m*-CNB/*p*-CNB selectivity of SiO₂ and glass bead is less than one as adsorption capacity of *m*-CNB is lower than *p*-CNB (Leardsakulthong, 2008).

Table 4.1 Selectivity and adsorption capacities of *m*-CNB and *p*-CNB on various adsorbents

Adsorbent	<i>m</i> -CNB/ <i>p</i> -CNB selectivity	Adsorption capacity (g/g adsorbent)	
		<i>m</i> -CNB	<i>p</i> -CNB
NaX	1.12	7.61×10^{-2}	6.81×10^{-2}
CaX	1.17	8.00×10^{-2}	6.83×10^{-2}
BaX	1.32	1.24×10^{-2}	0.94×10^{-2}
NaY	1.40	2.49×10^{-2}	1.78×10^{-2}
CaY	2.08	5.08×10^{-2}	2.44×10^{-2}
KY	1.49	0.98×10^{-2}	0.66×10^{-2}
SiO ₂	0.96	0.98×10^{-2}	1.02×10^{-2}
Al ₂ O ₃	1.01	1.77×10^{-2}	1.75×10^{-2}
Activated carbon	0.96	10.21×10^{-2}	10.68×10^{-2}
Glass bead	0.91	0.48×10^{-2}	0.52×10^{-2}

4.2 Effects of Feed Composition on the *m*- and *p*-CNB Crystallization

For this part, effects of feed compositions on the *m*-CNB and *p*-CNB crystallization were investigated. The feed compositions at 61.0, 62.9, and 63.5 wt% *m*-CNB were used without any adsorbent to investigate crystal compositions and temperatures that the crystals were formed. Seven grams of solid *m*- and *p*-CNB were melted to obtain a homogeneous liquid solution. The liquid mixture was measured for the CNB compositions by the GC. Then, the liquid mixture in the crystallizer was cooled by the cooling water from 30°C to a crystallization temperature. All crystals were collected from the crystallizer, washed, and dissolved with hexane. The dissolved crystals were measured for the CNB compositions by the GC. The CNB compositions with different starting liquid mixtures without any adsorbent are shown in Table 4.2.

Table 4.2 Composition of *m*- and *p*-CNB in the feeds and crystals, and crystallization temperatures

Feed	Feed composition (wt%)		Precipitate composition (wt%)		Crystallization temperature (°C)
	<i>m</i> -CNB	<i>p</i> -CNB	<i>m</i> -CNB	<i>p</i> -CNB	
Below the eutectic composition	61.02	38.98	9.60	90.40	23.0
At the eutectic composition	62.90	37.10	62.87	37.13	23.0
Above the eutectic composition	63.50	36.50	84.77	15.23	23.3

Without any adsorbent, the result shows that the precipitates appear in a crystal form with 61 wt% *m*-CNB (below the eutectic composition) and 63.5 wt% *m*-CNB (above the eutectic composition) in the feed. However, the precipitate from 62.9 wt% *m*-CNB (at the eutectic composition) in the feed is an amorphous solid with the composition close to that of the original feed. Below the eutectic composition, the crystals are rich in *p*-CNB, 90.40 wt%. Above the eutectic composition, the crystals are rich in *m*-CNB, 84.77 wt%. The precipitate composition and crystallization temperature at each feed composition are shown in Table 4.2. These results conform to the binary phase diagram as shown in Figure 4.1. In any case, 100 wt% pure crystals cannot be produced by a single crystallization for many reasons. For example, the impurities or residual solvent that have not been removed by washing can contaminate the crystal. In addition, these impurities can occur by inclusion of mother liquor into the crystal and by its adhesion on the crystal surfaces (Mullin, 2001; Funakoshi *et al.*, 2001).

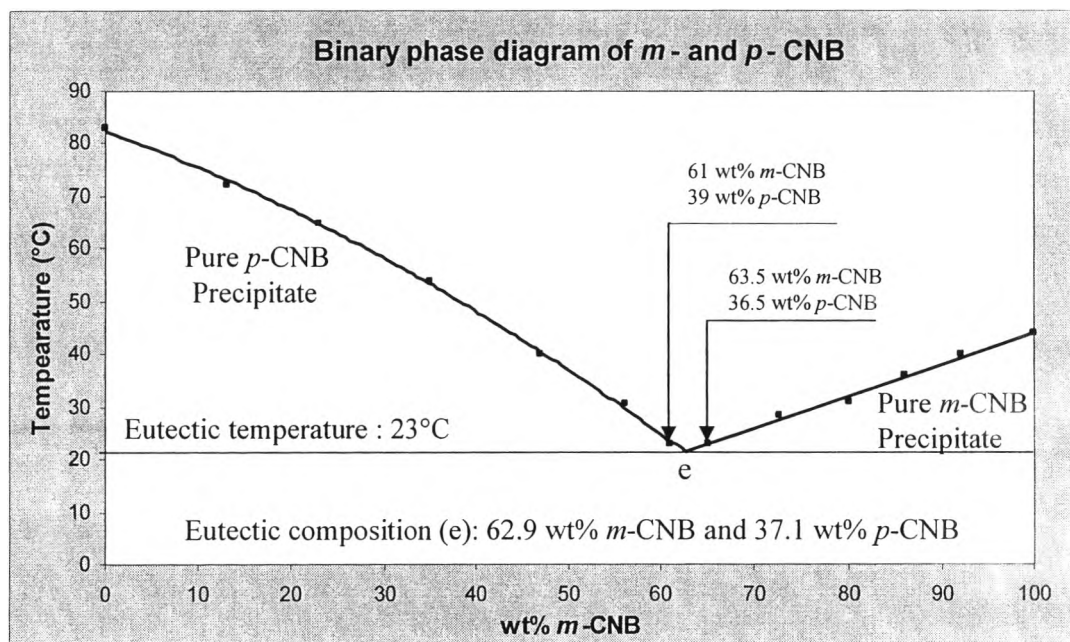


Figure 4.1 Binary phase diagram of *m*- and *p*-CNB (Sulzer Chemtech Pte., Ltd).

4.3 Effects of Adsorbents on the Crystallization and Composition of *m*- and *p*-CNB

4.3.1 Effects of Adsorbents on the CNB Feed Solution Compositions

To study the effects of the adsorbents on the feed composition, experiments were carried out at and above the eutectic composition (62.9 and 63.5 wt% *m*-CNB in the feed, respectively). At the eutectic composition, 7 grams of 0.629 and 0.371 mass fractions of *m*-CNB and *p*-CNB, respectively, was melted to obtain a homogeneous liquid mixture. The adsorbents were calcined at 350°C for an hour before adding into the CNB mixture. After 3 hrs, the mixture was stirred to minimize any concentration gradient in the solution. Then, the mixture compositions after adding adsorbents as shown in Tables 4.3, 4.4, and 4.5 were determined by the GC. The experiment was repeated by using 63.5 wt% *m*-CNB in the feed and varying number of adsorbents (5 and 10 grains). The feed compositions before and after adding the adsorbents are almost the same; therefore, it may be concluded that the type and number of the adsorbents do not significantly affect the feed composition. It

seems that the adsorbents act like a nucleating agent more than adsorbing CNB compositions.

Table 4.3 *m*- and *p*-CNB composition in the feed with 62.9 wt% of *m*-CNB before and after adding 5 grains of adsorbents at 30°C

Adsorbent	Feed composition before adding adsorbent (wt%)		Feed composition after adding adsorbent (wt%)		% difference*
	<i>m</i> -CNB	<i>p</i> -CNB	<i>m</i> -CNB	<i>p</i> -CNB	
NaX	62.91	37.09	62.90	37.10	-0.01
CaX	62.96	37.04	62.90	37.10	-0.06
BaX	62.94	37.06	62.92	37.08	-0.02
NaY	62.95	37.05	62.93	37.07	-0.02
CaY	62.91	37.09	62.93	37.07	+0.02
KY	62.92	37.08	62.91	37.09	-0.01
SiO ₂	62.90	37.10	62.89	37.11	-0.01
Al ₂ O ₃	62.91	37.09	62.89	37.11	-0.02
Activated carbon	62.93	37.07	62.94	37.06	-0.01
Glass bead	62.92	37.08	61.90	37.10	-0.02

* %difference is the difference between the *m*-CNB composition in the feed with and without adsorbent.

Table 4.4 *m*- and *p*-CNB composition in the feed with 63.5 wt% of *m*-CNB before and after adding 5 grains of adsorbents at 30°C

Adsorbent	Feed composition before adding adsorbent (wt%)		Feed composition after adding adsorbent (wt%)		% difference*
	<i>m</i> -CNB	<i>p</i> -CNB	<i>m</i> -CNB	<i>p</i> -CNB	
NaX	63.46	36.54	63.49	36.51	-0.03
CaX	63.54	36.46	63.58	36.42	+0.04
BaX	63.48	36.52	63.42	36.58	-0.06
NaY	63.55	36.45	63.56	36.44	+0.01
CaY	63.54	36.46	63.60	36.40	+0.06
KY	63.51	36.49	63.54	36.46	+0.03
SiO ₂	63.49	36.51	63.52	36.48	+0.03
Al ₂ O ₃	63.53	36.47	63.49	36.51	+0.04
Activated carbon	63.52	36.48	63.50	36.50	+0.02
Glass bead	63.47	36.53	63.51	36.49	+0.04

* %difference is the difference between the *m*-CNB composition in the feed with and without adsorbent.

Table 4.5 *m*- and *p*-CNB composition in the feed with 63.5 wt% of *m*-CNB before and after adding 10 grains of adsorbents at 30°C

Adsorbent	Feed composition before adding adsorbent (wt%)		Feed composition after adding adsorbent (wt%)		% difference*
	<i>m</i> -CNB	<i>p</i> -CNB	<i>m</i> -CNB	<i>p</i> -CNB	
NaX	63.51	36.49	63.46	36.54	-0.05
CaX	63.49	36.51	63.46	36.54	-0.03
BaX	63.48	36.52	63.42	36.58	-0.06
NaY	63.55	36.45	63.56	36.44	+0.01
CaY	63.54	36.46	63.60	36.40	+0.06
KY	63.51	36.49	63.42	36.58	-0.09
SiO ₂	63.54	36.46	63.49	36.51	-0.05
Al ₂ O ₃	63.52	36.48	63.49	36.51	-0.03
Activated carbon	63.54	36.46	63.53	36.47	-0.01
Glass bead	63.45	36.55	63.52	36.48	+0.07

* %difference is the difference between the *m*-CNB composition in the feed with and without adsorbent.

4.3.2 Effects of Adsorbents on the CNB Crystal Composition and Crystallization Temperature

The CNB mixture with 5 grains of an adsorbent was cooled by cooling water at the cooling rate of 1°C/hr from 30°C until crystals were formed. The crystals were collected, washed, and dissolved with hexane. The CNB crystal composition was measured by the GC. The crystals were collected from 8 positions in two areas; the 1-4 positions near the adsorbents (area (a)) and the 5-8 position far from the adsorbents (area (b)) as shown in Figure 4.2.

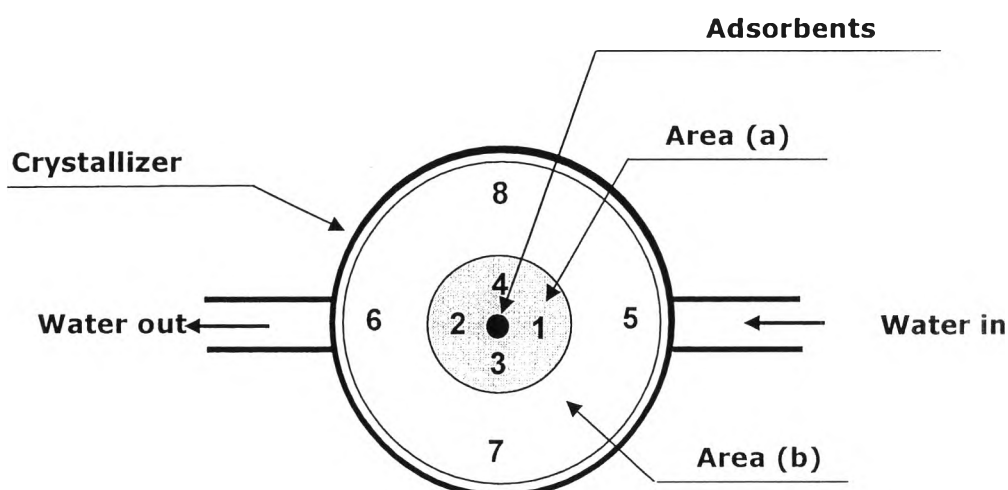


Figure 4.2 Locations where crystals were collected for *m*- and *p*-CNB composition analysis.

From Tables 4.6, the presence of the adsorbents in the system at the eutectic composition (62.9 wt% *m*-CNB in the feed) results in the crystal formation instead of amorphous, and the crystal compositions are rich in *p*-CNB. It can be clearly seen that the crystals near the adsorbents (area(a)) have *p*-CNB purity higher than those far from the adsorbents (area(b)).

Table 4.6 Composition of *m*- and *p*-CNB in the crystals located near and far from adsorbents with 62.9 wt% of *m*-CNB in the feed and 5 grains of adsorbents

Adsorbent	Crystal near adsorbent			Crystal far from adsorbent		
	Composition (wt%)			Composition (wt%)		
	<i>m</i> -CNB	<i>p</i> -CNB	<i>m</i> / <i>p</i> -CNB	<i>m</i> -CNB	<i>p</i> -CNB	<i>m</i> / <i>p</i> -CNB
NaX	5.19 [1]	94.81 [1]	0.0547	9.88 [5]	90.12 [5]	0.1096
	5.95 [2]	94.05 [2]	0.0633	8.19 [6]	91.81 [6]	0.0892
	5.91 [3]	94.09 [3]	0.0628	10.02 [7]	89.98 [7]	0.1114
	5.89 [4]	94.11 [4]	0.0626	9.87 [8]	90.13 [8]	0.1095
CaX	8.89 [1]	91.11 [1]	0.0976	13.19 [5]	86.81 [5]	0.1519
	9.68 [2]	90.32 [2]	0.1072	12.08 [6]	87.92 [6]	0.1374
	9.41 [3]	90.59 [3]	0.1039	14.75 [7]	85.25 [7]	0.1730
	8.82 [4]	91.18 [4]	0.0967	14.83 [8]	85.17 [8]	0.1741
BaX	8.31 [1]	91.69 [1]	0.0906	10.06 [5]	89.94 [5]	0.1119
	5.11 [2]	94.89 [2]	0.0539	12.50 [6]	87.50 [6]	0.1429
	7.70 [3]	92.30 [3]	0.0834	12.30 [7]	87.70 [7]	0.1403
	7.00 [4]	93.00 [4]	0.0753	12.30 [8]	87.70 [8]	0.1403
NaY	3.79 [1]	96.21 [1]	0.0394	5.59 [5]	94.41 [5]	0.0592
	4.97 [2]	95.03 [2]	0.0523	10.46 [6]	89.54 [6]	0.1168
	3.95 [3]	96.05 [3]	0.0411	3.97 [7]	96.03 [7]	0.0413
	5.35 [4]	94.65 [4]	0.0565	11.07 [8]	88.93 [8]	0.1245
CaY	5.07 [1]	94.93 [1]	0.0534	11.02 [5]	88.98 [5]	0.1238
	4.18 [2]	95.82 [2]	0.0436	5.75 [6]	94.24 [6]	0.0611
	4.46 [3]	95.54 [3]	0.0467	4.72 [7]	95.28 [7]	0.0495
	4.44 [4]	95.56 [4]	0.0465	6.16 [8]	93.84 [8]	0.0656
KY	4.02 [1]	95.98 [1]	0.0419	4.06 [5]	95.94 [5]	0.0423
	3.99 [2]	96.01 [2]	0.0416	4.06 [6]	95.94 [6]	0.0423
	3.98 [3]	96.02 [3]	0.0414	4.32 [7]	95.68 [7]	0.0452
	3.82 [4]	96.18 [4]	0.0397	5.22 [8]	94.78 [8]	0.0551

* The number in the parenthesis refers to the position where crystals were collected as shown in Figure 4.2.

Table 4.6 (cont.) Composition of *m*- and *p*-CNB in the crystals located near and far from adsorbents with 62.9 wt% of *m*-CNB in the feed and 5 grains of adsorbents

Adsorbent	Crystal near adsorbent			Crystal far from adsorbent		
	Composition (wt%)			Composition (wt%)		
	<i>m</i> -CNB	<i>p</i> -CNB	<i>m</i> -/ <i>p</i> -CNB	<i>m</i> -CNB	<i>p</i> -CNB	<i>m</i> -/ <i>p</i> -CNB
SiO ₂	3.28 [1]	96.72 [1]	0.0339	12.66 [5]	87.34 [5]	0.1450
	4.04 [2]	95.96 [2]	0.0421	10.79 [6]	89.21 [6]	0.1210
	4.54 [3]	95.46 [3]	0.0476	13.53 [7]	86.47 [7]	0.1565
	5.36 [4]	94.64 [4]	0.0566	12.14 [8]	87.86 [8]	0.1382
Al ₂ O ₃	3.97 [1]	96.03 [1]	0.0413	13.61 [5]	86.39 [5]	0.1575
	3.87 [2]	96.13 [2]	0.0403	15.43 [6]	84.57 [6]	0.1825
	4.86 [3]	95.14 [3]	0.0511	10.43 [7]	89.57 [7]	0.1164
	5.75 [4]	94.25 [4]	0.0610	8.78 [8]	91.22 [8]	0.0963
Activated carbon	6.49 [1]	93.51 [1]	0.0694	12.27 [5]	87.73 [5]	0.1399
	6.77 [2]	93.23 [2]	0.0726	9.95 [6]	90.05 [6]	0.1105
	5.55 [3]	94.45 [3]	0.0588	11.87 [7]	88.13 [7]	0.1347
	6.21 [4]	93.79 [4]	0.0662	9.88 [8]	90.12 [8]	0.1096
Glass bead	6.76 [1]	93.24 [1]	0.0725	13.82 [5]	86.18 [5]	0.1604
	7.31 [2]	92.69 [2]	0.0789	12.07 [6]	87.93 [6]	0.1373
	6.83 [3]	93.17 [3]	0.0733	13.56 [7]	86.44 [7]	0.1569
	4.86 [4]	95.14 [4]	0.0511	11.87 [8]	88.13 [8]	0.1347

* The number in the parenthesis refers to the position where crystals were collected as shown in Figure 4.2.

In order to see the tendency of crystal compositions clearly, the CNB crystal compositions in the feed solution at the eutectic composition was calculated in terms of *m*-/*p*-CNB ratio, as seen in Figures 4.3. The results show that the crystallization gives almost the same *m*-/*p*-CNB ratio of the crystals at the locations near the adsorbent, while the *m*-/*p*-CNB ratio at the locations far from the adsorbent shows some dependency on the type of the adsorbents. Moreover, the presence of the adsorbent can induce nucleation at a temperature lower than that required for crystallization without any adsorbent, as shown in Table 4.7.

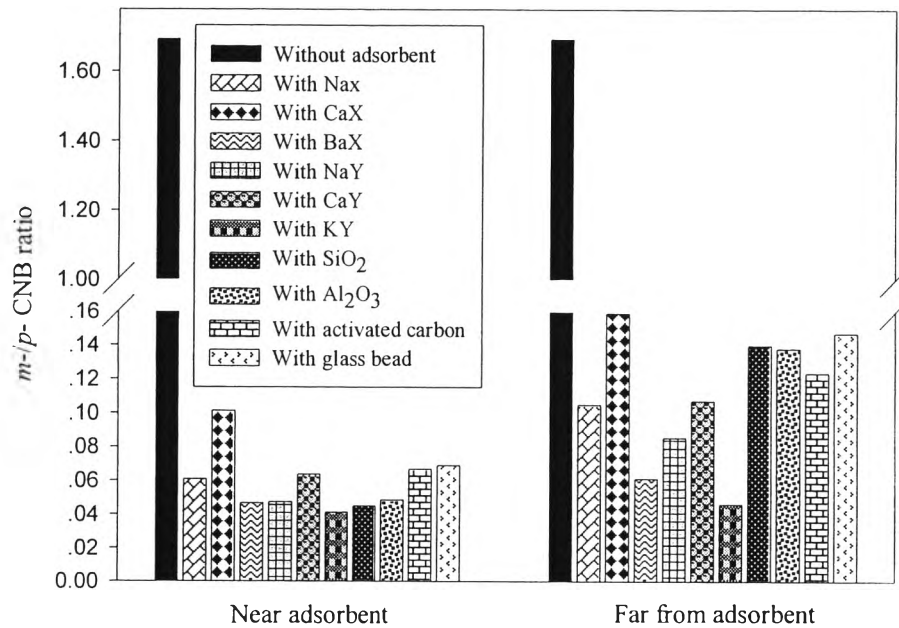


Figure 4.3 Comparison of m/p -CNB ratio of the precipitate with 62.9 wt% of m -CNB in the feed (at the eutectic composition) and 5 grains of adsorbent.

Table 4.7 Crystallization temperatures of 62.9 wt% of m -CNB in the feed with 5 grains of adsorbents

Type of adsorbent	Crystallization Temperature (°C)
	5 grains of adsorbent
Without adsorbent	23.0
NaX	21.0
CaX	21.0
BaX	19.5
NaY	21.0
CaY	20.0
KY	21.0
SiO ₂	19.0
Al ₂ O ₃	21.0
Activated carbon	21.0
Glass bead	20.0

4.3.3 Effects of the Number of Adsorbents on the CNB Crystal Compositions and Crystallization Temperature

The influence of the number of adsorbents on the crystallization was also studied by varying the number of adsorbents (5 and 10 grains) and carried out at 63.5 wt% of *m*-CNB in the feed. The CNB liquid mixture was prepared with the same procedure as that at the eutectic composition. The crystals were collected from 8 positions in two areas, area (a) (the 1-4 positions near the adsorbents) and area (b) (the 5-8 positions far from the adsorbents). The results are shown in Tables 4.8 and 4.9, the presence of adsorbents in the feed above the eutectic composition can shift the crystal composition from being rich in *m*-CNB to rich in *p*-CNB, and the crystals near the adsorbents have *p*-CNB purity higher than those far from the adsorbent as shown in Figures 4.4 and 4.5. From Table 4.10, the presence of the adsorbent can induce nucleation at a temperature lower than that required for crystallization without any adsorbent, and that is true for both 5 and 10 grains of adsorbents.

Table 4.8 Composition of *m*- and *p*-CNB in the crystals located near and far from adsorbents with 63.5 wt% of *m*-CNB in the feed and 5 grains of adsorbents

Adsorbent	Crystal near adsorbent			Crystal far from adsorbent		
	Composition (wt%)			Composition (wt%)		
	<i>m</i> -CNB	<i>p</i> -CNB	<i>m/p</i> -CNB	<i>m</i> -CNB	<i>p</i> -CNB	<i>m/p</i> -CNB
NaX	3.77 [1]	96.23 [1]	0.0392	4.78 [5]	95.22 [5]	0.0502
	4.53 [2]	95.47 [2]	0.0474	4.74 [6]	95.26 [6]	0.0498
	4.27 [3]	95.73 [3]	0.0446	4.87 [7]	95.13 [7]	0.0512
	4.22 [4]	95.78 [4]	0.0441	4.27 [8]	95.73 [8]	0.0446
CaX	4.13 [1]	95.87 [1]	0.0431	10.09 [5]	89.91 [5]	0.1122
	5.82 [2]	94.18 [2]	0.0618	12.22 [6]	87.78 [6]	0.1392
	6.56 [3]	93.44 [3]	0.0702	12.67 [7]	87.33 [7]	0.1451
	5.62 [4]	94.38 [4]	0.0595	14.11 [8]	85.89 [8]	0.1643
BaX	5.38 [1]	94.62 [1]	0.0569	6.18 [5]	93.82 [5]	0.0659
	4.36 [2]	95.64 [2]	0.0456	5.23 [6]	94.77 [6]	0.0552
	5.23 [3]	94.77 [3]	0.0552	6.66 [7]	93.34 [7]	0.0714
	4.86 [4]	95.14 [4]	0.0511	4.95 [8]	95.05 [8]	0.0521
NaY	6.98 [1]	93.02 [1]	0.0750	9.46 [5]	90.54 [5]	0.1045
	4.75 [2]	95.25 [2]	0.0499	10.23 [6]	89.77 [6]	0.1140
	4.82 [3]	95.18 [3]	0.0506	11.35 [7]	88.65 [7]	0.1280
	6.05 [4]	93.95 [4]	0.0644	8.82 [8]	91.18 [8]	0.0967
CaY	6.05 [1]	93.95 [1]	0.0644	9.88 [5]	90.12 [5]	0.1096
	6.02 [2]	93.98 [2]	0.0641	9.47 [6]	90.53 [6]	0.1046
	5.59 [3]	94.41 [3]	0.0592	9.52 [7]	90.48 [7]	0.1052
	6.27 [4]	93.73 [4]	0.0669	9.88 [8]	90.12 [8]	0.1096
KY	4.55 [1]	95.45 [1]	0.0477	5.20 [1]	94.80 [1]	0.0549
	4.11 [2]	95.89 [2]	0.0429	4.86 [2]	95.14 [2]	0.0511
	4.44 [3]	95.56 [3]	0.0465	4.71 [3]	95.29 [3]	0.0494
	3.90 [4]	96.10 [4]	0.0406	4.01 [4]	95.99 [4]	0.0418

* The number in the parenthesis refers to the position where crystals were collected as shown in Figure 4.2.

Table 4.8 (cont.) Composition of *m*- and *p*-CNB in the crystals located near and far from adsorbents with 63.5 wt% of *m*-CNB in the feed and 5 grains of adsorbents

Adsorbent	Crystal near adsorbent			Crystal far from adsorbent		
	Composition (wt%)			Composition (wt%)		
	<i>m</i> -CNB	<i>p</i> -CNB	<i>m</i> / <i>p</i> -CNB	<i>m</i> -CNB	<i>p</i> -CNB	<i>m</i> / <i>p</i> -CNB
SiO ₂	4.75 [1]	95.25 [1]	0.0499	8.18 [5]	91.82 [5]	0.0891
	5.83 [2]	94.17 [2]	0.0619	9.89 [6]	90.11 [6]	0.1098
	5.17 [3]	94.83 [3]	0.0545	10.47 [7]	89.53 [7]	0.1169
	6.02 [4]	93.98 [4]	0.0641	10.21 [8]	89.79 [8]	0.1137
Al ₂ O ₃	4.53 [1]	95.47 [1]	0.0474	6.44 [5]	93.56 [5]	0.069
	4.38 [2]	95.62 [2]	0.0458	4.94 [6]	95.06 [6]	0.0520
	4.36 [3]	95.64 [3]	0.0456	4.93 [7]	95.07 [7]	0.0519
	4.10 [4]	95.90 [4]	0.0428	5.14 [8]	94.86 [8]	0.0542
Activated carbon	6.30 [1]	93.70 [1]	0.0672	8.28 [5]	91.72 [5]	0.0903
	4.21 [2]	95.79 [2]	0.0440	6.73 [6]	93.27 [6]	0.0722
	6.27 [3]	93.73 [3]	0.0669	6.67 [7]	93.33 [7]	0.0715
	4.93 [4]	95.07 [4]	0.0519	5.60 [8]	94.40 [8]	0.0593
Glass bead	6.11 [1]	93.89 [1]	0.0651	6.62 [5]	93.38 [5]	0.0709
	4.25 [2]	95.75 [2]	0.0444	4.24 [6]	95.76 [6]	0.0443
	4.69 [3]	95.31 [3]	0.0492	4.39 [7]	95.61 [7]	0.0459
	5.13 [4]	94.87 [4]	0.0541	6.10 [8]	93.90 [8]	0.0650

* The number in the parenthesis refers to the position where crystals were collected as shown in Figure 4.2.

Table 4.9 Composition of *m*- and *p*-CNB in the crystals located near and far from adsorbents with 63.5 wt% of *m*-CNB in the feed and 10 grains of adsorbents

Adsorbent	Crystal near adsorbent			Crystal far from adsorbent		
	Composition (wt%)			Composition (wt%)		
	<i>m</i> -CNB	<i>p</i> -CNB	<i>m</i> -/ <i>p</i> -CNB	<i>m</i> -CNB	<i>p</i> -CNB	<i>m</i> -/ <i>p</i> -CNB
NaX	4.44 [1]	95.56 [1]	0.0465	6.22 [5]	93.78 [5]	0.0663
	3.37 [2]	96.63 [2]	0.0349	4.97 [6]	95.03 [6]	0.0523
	3.84 [3]	96.16 [3]	0.0399	5.19 [7]	94.81 [7]	0.0547
	4.32 [4]	95.68 [4]	0.0452	5.30 [8]	94.70 [8]	0.0560
CaX	5.64 [1]	94.36 [1]	0.0598	7.96 [5]	92.04 [5]	0.0865
	3.76 [2]	96.24 [2]	0.0391	5.54 [6]	94.46 [6]	0.0586
	4.58 [3]	95.42 [3]	0.0480	4.92 [7]	95.08 [7]	0.0517
	4.60 [4]	95.40 [4]	0.0482	5.48 [8]	94.52 [8]	0.0580
BaX	3.61 [1]	96.39 [1]	0.0375	4.93 [5]	95.07 [5]	0.0519
	3.63 [2]	96.37 [2]	0.0377	4.65 [6]	95.35 [6]	0.0488
	4.00 [3]	96.00 [3]	0.0417	4.74 [7]	95.26 [7]	0.0498
	3.95 [4]	96.05 [4]	0.0411	4.08 [8]	95.92 [8]	0.0425
NaY	3.95 [1]	96.05 [1]	0.0411	4.13 [5]	95.87 [5]	0.0431
	3.84 [2]	96.16 [2]	0.0399	3.90 [6]	96.10 [6]	0.0406
	3.84 [3]	96.16 [3]	0.0399	4.09 [7]	95.91 [7]	0.0426
	3.96 [4]	96.04 [4]	0.0412	5.59 [8]	94.41 [8]	0.0592
CaY	4.26 [1]	95.74 [1]	0.0445	5.56 [5]	94.44 [5]	0.0589
	8.70 [2]	91.30 [2]	0.0953	8.74 [6]	91.26 [6]	0.0958
	7.97 [3]	92.03 [3]	0.0866	9.44 [7]	90.56 [7]	0.1042
	5.11 [4]	94.89 [4]	0.0539	9.23 [8]	90.77 [8]	0.1017
KY	4.35 [1]	95.65 [1]	0.0455	5.16 [5]	94.84 [5]	0.0544
	3.68 [2]	96.32 [2]	0.0382	4.11 [6]	95.89 [6]	0.0429
	3.58 [3]	96.42 [3]	0.0371	3.82 [7]	96.18 [7]	0.0397
	3.62 [4]	96.38 [4]	0.0376	4.54 [8]	95.46 [8]	0.0476

* The number in the parenthesis refers to the position where crystals were collected as shown in Figure 4.2.

Table 4.9 (cont.) Composition of *m*- and *p*-CNB in the crystals located near and far from adsorbents with 63.5 wt% of *m*-CNB in the feed and 10 grains of adsorbents

Adsorbent	Crystal near adsorbent			Crystal far from adsorbent		
	Composition (wt%)			Composition (wt%)		
	<i>m</i> -CNB	<i>p</i> -CNB	<i>m</i> -/ <i>p</i> -CNB	<i>m</i> -CNB	<i>p</i> -CNB	<i>m</i> -/ <i>p</i> -CNB
SiO ₂	4.35 [1]	95.65 [1]	0.0455	5.46 [5]	94.54 [5]	0.0578
	4.93 [2]	95.07 [2]	0.0519	5.23 [6]	94.77 [6]	0.0552
	4.00 [3]	96.00 [3]	0.0417	4.84 [7]	95.16 [7]	0.0509
	4.06 [4]	95.94 [4]	0.0423	4.46 [8]	95.54 [8]	0.0467
Al ₂ O ₃	4.43 [1]	95.57 [1]	0.0464	5.44 [5]	94.56 [5]	0.0575
	3.96 [2]	96.04 [2]	0.0412	4.32 [6]	95.68 [6]	0.0452
	4.18 [3]	95.82 [3]	0.0436	4.33 [7]	95.67 [7]	0.0453
	3.92 [4]	96.08 [4]	0.0408	4.31 [8]	95.69 [8]	0.0450
Activated carbon	4.14 [1]	95.86 [1]	0.0432	7.01 [5]	92.99 [5]	0.0754
	3.90 [2]	96.10 [2]	0.0406	4.00 [6]	96.00 [6]	0.0417
	4.19 [3]	95.81 [3]	0.0437	5.67 [7]	94.33 [7]	0.0601
	4.12 [4]	95.88 [4]	0.0430	4.70 [8]	95.30 [8]	0.0493
Glass bead	4.06 [1]	95.94 [1]	0.0423	4.54 [5]	95.46 [5]	0.0476
	3.87 [2]	96.13 [2]	0.0403	4.03 [6]	95.97 [6]	0.0420
	4.13 [3]	95.87 [3]	0.0431	4.26 [7]	95.74 [7]	0.0445
	4.08 [4]	95.92 [4]	0.0425	4.22 [8]	95.78 [8]	0.0441

* The number in the parenthesis refers to the position where crystals were collected as shown in Figure 4.2.

Table 4.10 Crystallization temperatures at 63.5 wt% of *m*-CNB in the feed with 5 and 10 grains of adsorbents

Adsorbent	Crystallization Temperature (°C)	
	5 grains of adsorbent	10 grains of adsorbent
Without adsorbent	23.3	23.3
NaX	19.5	20.5
CaX	17.5	20.5
BaX	19.0	20.0
NaY	19.0	20.0
CaY	17.0	20.5
KY	19.0	20.0
SiO ₂	19.5	20.5
Al ₂ O ₃	19.0	20.5
Activated carbon	20.0	20.0
Glass bead	19.0	20.5

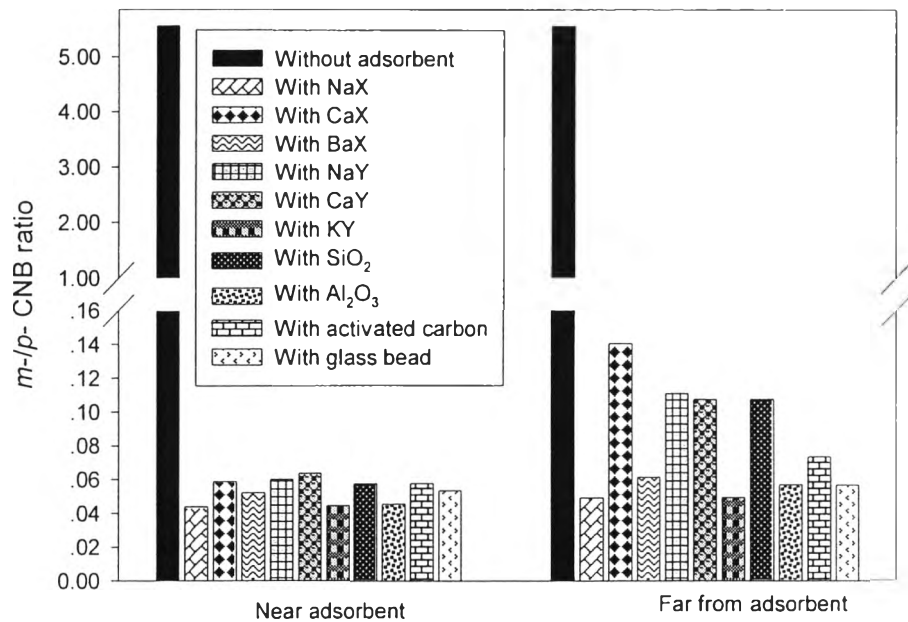


Figure 4.4 Comparison of m/p -CNB ratio of the precipitates with 63.5 wt% m -CNB in the feed and 5 grains of adsorbents (NaX, CaX, BaX, NaY, CaY, KY, SiO₂, Al₂O₃, activated carbon, and glass bead).

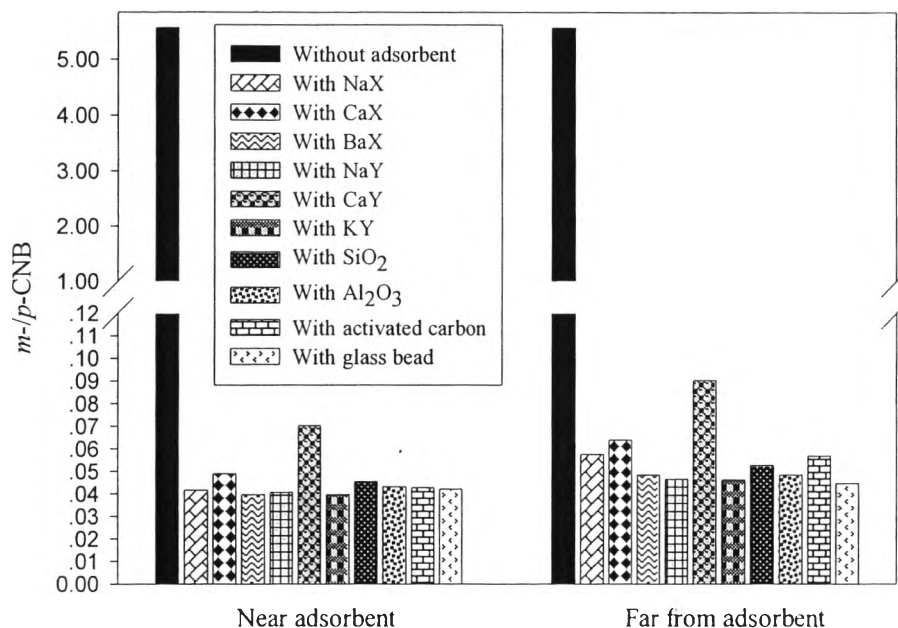


Figure 4.5 Comparison of $m-/p$ -CNB ratio of the precipitates with 63.5 wt% m -CNB in the feed and 10 grains of adsorbents (NaX, CaX, BaX, NaY, CaY, KY, SiO₂, Al₂O₃, activated carbon, and glass bead).

When an adsorbent is added into the CNB mixture, it may act as a foreign particle or insoluble impurity in the system. In the nucleation step, the effect of insoluble impurity is unpredictable; however, it can influence crystal growth rates in a variety of ways. It can change the properties of the solution (structure or otherwise) or the equilibrium saturation concentration and hence the supersaturation. It can alter the characteristics of the adsorption layer at the crystal-solution interface and influence the integration of growth units. It may be built into the crystal, especially if there is some degree of lattice similarity so the reason why the crystal composition at the eutectic composition in the feed is changed from amorphous form to rich p -CNB crystal form may be related with the adsorption layer at the p -CNB crystal-solution interface alteration property of adsorbent (Mullin, 2001). This effect may change characteristics of adsorption layer into p -CNB crystal selection layer. Another reason may be that the presence of an adsorbent may induce primary nucleation in the heterogeneous nucleation. The size of a foreign body is important,

and there is an evidence to suggest that the most active particle (heteronuclei) in liquid solution lie in the range 0.1 to 1 μm . The adsorbent that has an average particle size diameter more than 1 μm can considerably affect heterogeneous nucleation, which usually has a profound effect on the final crystalline product (Mullin, 2001).

A reason why the number of an adsorbent significantly impacts on product purity may come from the agglomeration of nuclei in the nucleation step. The agglomeration kinetics is correlated as a function of the number of particles and the supersaturation in the solution (Funakoshi *et al.*, 2001). The nuclei in the primary nucleation from the induction by foreign particles are called heterogeneous nuclei. From Table 4.10, the crystallization temperature in the presence of 5 grains of adsorbents is slightly lower than that with 10 grains. It may be possible that 10 grains of adsorbent can induce higher the number of heterogeneous nuclei than 5 grains of adsorbents, and the crystal growth rate of CNBs in the presence of 10 grains in the system is higher than that with 5 grains; hence, decrease the agglomeration time leading to the higher *p*-CNB purity as shown in Figure 4.6.

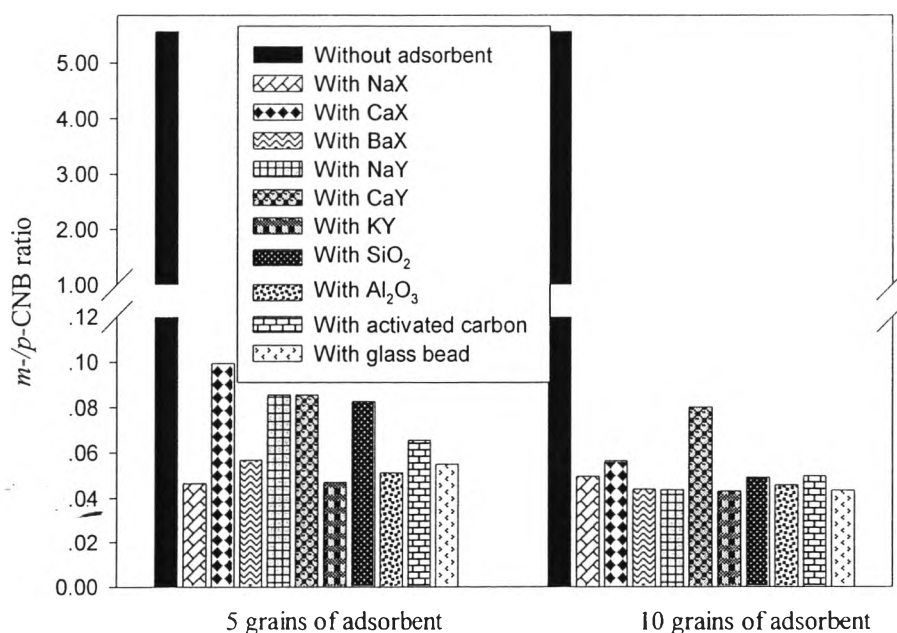


Figure 4.6 Effects of the number adsorbents on *m*-/*p*-CNB ratio of the crystals at 63.5 wt% *m*-CNB in the feed.

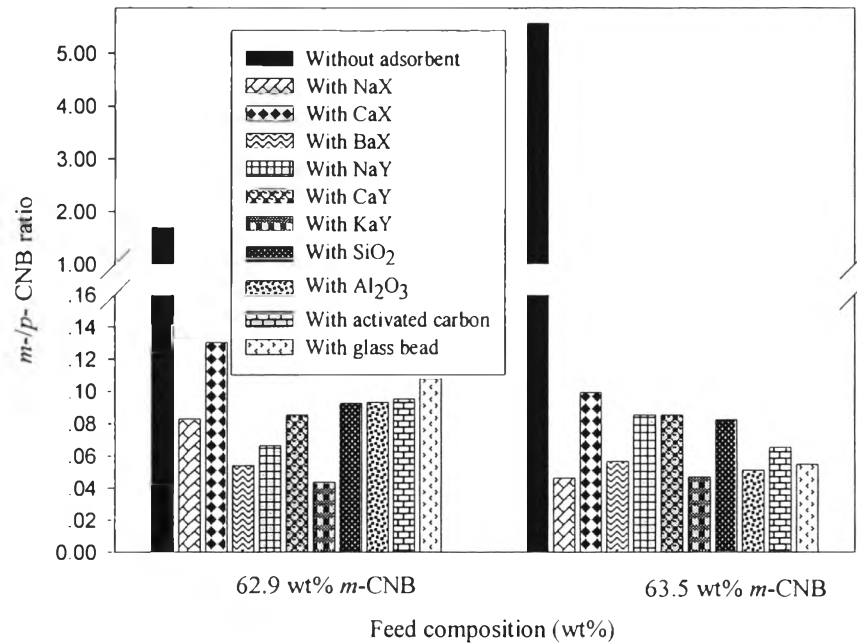


Figure 4.7 Comparison of m/p -CNB ratio of the precipitates with 62.9 and 63.5 wt% m -CNB in the feed and 5 grains of adsorbents (NaX, CaX, BaX, NaY, CaY, KY, SiO₂, Al₂O₃, activated carbon, and glass bead).

From Figure 4.7, possible reasons why the presence of adsorbent at the eutectic composition in the feed can shift from amorphous solid to rich in p -CNB crystals form, whereas the composition of the precipitates obtained from the feed above the eutectic composition is shifted from being rich m -CNB to rich in p -CNB may come from the metastable zone width, interfacial tension, and structure change of solution. As a result of the presence of an adsorbent in the CNB mixture, the crystallization temperature is lower than that in the system without any adsorbent. The metastable zone width is explained by the solubility-supersolubility diagram as shown in Figure 4.8 for interfacial tension associates with the overall free energy change under heterogeneous conditions $\Delta G'_{\text{crit}}$ and the overall free energy change under homogeneous nucleation ΔG_{crit} .

The relationship between supersaturation and spontaneous crystallization led to a diagrammatic representation of the metastable zone on a

solubility-supersolubility diagram as shown in Figure 4.8. The lower continuous solubility curve can be located with precision. The upper broken supersolubility curve, which represents temperatures and concentrations, at which uncontrolled spontaneous crystallization occurs, is not as well defined as that of the solubility curve. Its position in the diagram is considerably affected by, amongst other things, the rate at which supersaturation is generated, the intensity of agitation, the presence of trace impurities and the thermal history of the solution. The diagram is divided into three zone (Mullin, 2001):

1. The stable (unsaturated) zone, where crystallization is impossible.
2. The metastable (supersaturated) zone, between the solubility and supersolubility curve, where spontaneous crystallization is impossible. However, if a crystal seed were placed in such a metastable solution, growth would occur on it.
3. The unstable or labile (supersaturated) zone, where spontaneous crystallization is possible, but not inevitable.

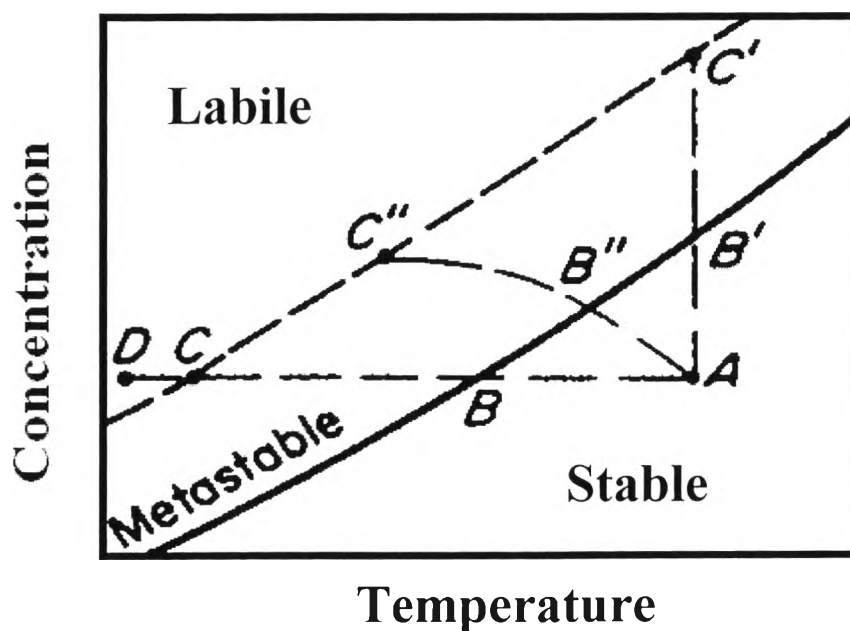


Figure 4.8 Solubility-supersolubility diagram (Mullin, 2001).

If a solution represented by point *A* in Figure 4.8 is cooled without loss of solvent (line *ABC*), spontaneous crystallization cannot occur until conditions represented by point *C* are reached. At this point, crystallization may be spontaneous or it may be induced by seeding, agitation or mechanical shock. Further cooling to some point *D* may be necessary before crystallization can be induced (Mullin, 2001). The position in the diagram is considerably effected by the presence of trace impurities (Mullin, 2001) so that the presence of adsorbent in the CNB mixture may change the position in the diagram as well.

The maximum allowable supersaturation, Δc_{\max} , may be expressed in terms of the maximum allowable undercooling, $\Delta\theta_{\max}$:

$$\Delta c_{\max} = \left(\frac{dc^*}{d\theta} \right) \Delta\theta_{\max} \quad (4.1)$$

As the presence of a suitable foreign body or ‘sympathic’ surface can induce nucleation at degree of supercooling lower than those required for spontaneous nucleation (Mullin, 2001). This sentence is consistent with crystallization temperature in the presence of adsorbent, which is lower than in the absence of adsorbent. When the degree of supercooling decreases, $\Delta\theta_{\max}$ and Δc_{\max} increase according to the relationship between $\Delta\theta_{\max}$ and Δc_{\max} in Equation (4.1). Increasing $\Delta\theta_{\max}$ and Δc_{\max} results in a broader metastable zone width.

The overall free energy change associated with the formation of a critical nucleus under heterogeneous conditions, $\Delta G'_{\text{crit}}$, must be less than the corresponding free energy change, ΔG_{crit} , associated with homogeneous nucleation, i.e. (Mullin, 2001).

$$\Delta G'_{\text{crit}} = \phi \Delta G_{\text{crit}} \quad (4.2)$$

where the factor ϕ is less than unity.

The interfacial tension, γ , is one of the important factors controlling the nucleation process. Figure 4.9 shows an interfacial energy diagram for three

phases in contact; in this case, however, the three phases are not the more familiar solid, liquid, and gas, but two solids and a liquid. The three interfacial tensions are denoted by γ_{cl} (between the solid crystalline phase, c, and the liquid l), γ_{sl} (between another foreign solid surface, s, and the liquid) and γ_{cs} (between the solid crystalline phase and foreign solid surface) (Mullin, 2001). Resolving these forces in a horizontal direction

$$\gamma_{sl} = \gamma_{cs} + \gamma_{cl} \cos\theta \quad (4.3)$$

or

$$\cos\theta = \frac{\gamma_{sl} - \gamma_{cs}}{\gamma_{cl}} \quad (4.4)$$

The angle, θ , of contact between the crystalline deposit and foreign solid surface, corresponds to the angle of wetting in liquid-solid system (Mullin, 2001).

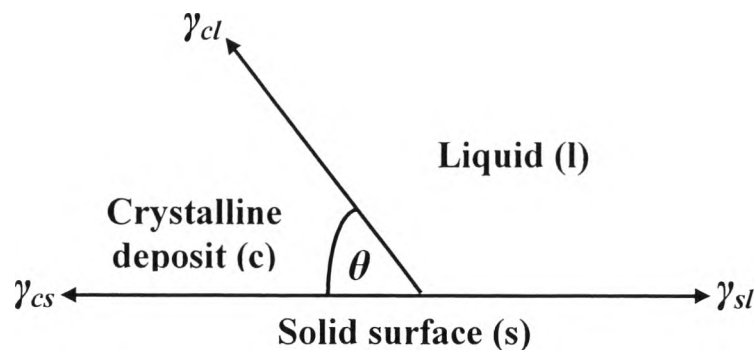


Figure 4.9 Interfacial tension at the boundaries between three phases (two solids, one liquid) (Mullin, 2001).

The factor ϕ in Equation 4.2 can be expressed as

$$\phi = \frac{(2 + \cos\theta)(1 - \cos\theta)^2}{4} \quad (4.5)$$

Thus, when $\theta=180^\circ$, $\cos\theta = -1$ and $\phi = 1$, Equation 4.2 becomes

$$\Delta G'_{\text{crit}} = \Delta G_{\text{crit}} \quad (4.6)$$

When θ lies between 0 and 180° , $\phi < 1$; therefore,

$$\Delta G'_{\text{crit}} < \Delta G_{\text{crit}} \quad (4.7)$$

When $\theta = 0$, $\phi = 0$, and

$$\Delta G'_{\text{crit}} = 0 \quad (4.8)$$

This is illustrated in Figure 4.10, which shows a foreign particle in a supersaturated solution (Mersmann, 2001).

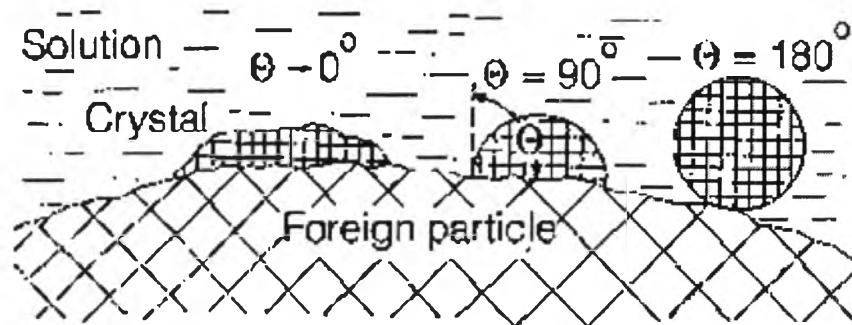


Figure 4.10 Nucleation on a foreign particle for different wetting angles (Mersmann, 2001).

For the cases of complete non-affinity between the crystalline solid and the foreign solid surface (corresponding to that of complete non-wetting in liquid-solid system), $\theta=180^\circ$, and Equation (4.6) applies, i.e. the overall free energy of nucleation is the same as that required for homogeneous or spontaneous nucleation. For the case partial affinity (cf. the partial wetting of a solid with a liquid), $0<\theta<180^\circ$, and Equation (4.7) applies, which indicates that nucleation is

easier to achieve because the overall excess free energy required is less than that for homogeneous nucleation. For the case of complete affinity (cf. complete wetting) $\theta=0$, and the free energy of nucleation of zero. This case corresponds to the seeding of a supersaturation solution with crystals of the required crystalline product, i.e. no nuclei have to be formed in the solution (Mullin, 2001).

The presence of an adsorbent may be in the case of the partial wetting of a solid with a liquid which is described by Equation (4.7), and ΔG_{crit} relate to $(\Delta T)^2$ as indicated in Equation (4.9).

$$\Delta G_{\text{crit}} \propto (\Delta T)^2 \quad (4.9)$$

where $\Delta T = T^* - T$ is the supercooling, T^* is the solid-liquid equilibrium temperature, and T is degree of supersaturation (Mullin, 2001).

From Equation (4.2), (4.7) and (4.9), the value of $\Delta G'_{\text{crit}}$ will be less than ΔG_{crit} when the value of ΔT is high that means the value of T or degree of supersaturation must be low. This relates to “The presence of a suitable foreign body or ‘sympathic’ surface can induce nucleation at degree of supercooling lower than those require for spontaneous nucleation (Mullin, 2001).” The metastable zone width may become broader. Thus, the crystallization temperature of the feed with the adsorbent decreases from the crystallization temperature of the feed without any adsorbent. The presence of the adsorbent may change the properties of the solution structure. The binary phase diagram of *m*- and *p*-CNB may be shifted to the right hand side. That is a reason why the precipitate composition in the feed at and above the eutectic composition is shifted from being rich in *m*-CNB to *p*-CNB (Mullin, 2001).